ISSN 2176-5480

In addition, in the technical literature different theories have been proposed to model the metal transfer mechanism. Among them, it can be mentioned the static force balance theory (SFBT) (Lancaster, 1986; Norrish, 1988; Amson, 1962; Amson, 1965; Waszink, *et. al.*, 1983), the Pinch Instability theory (PIT) (Allum, 1985a; Allum, 1985b; Lowke, 1997), the plasma force theory (PFT) (Needham, *et. al.*, 1960), the critical velocity theory (CVT) (Waszink and Van den Heuvel, 1982) and the dynamic force balance theory (DFBT) (Choi, *et. al.*, 2001; Jones, 1996; Jones, *et. al.*, 1988a; Jones, *et. al.*, 1988b; Watkins, *et. al.*, 1992), beyond the combinations those as SFBT and PIT (Kim, 1989; Kim and Eagar, 1993; Waszink and Piena, 1986), with limitations to assume constants thermophysics properties (Nemchinsky, 1998a; Nemchinsky, 1998b; Nemchinsky, 1998c). Recently, simulations have been conducted based on volume of fluid method (Vilarinho, 2002; Wang, *et. al.*, 2003; Fan and Kovacevic, 1999; Hirt, 1981; Haidar, 1998a; Haidar, 1998b; Choi, *et. al.*, 1999; Choi, *et. al.*, 1998a; Choi, *et. al.*, 1998b; Choi, *et. al.*, 1998c; Fan and Kovacevic, 1998).

It is also possible to identify models for GMAW process with more specific application or with distinct approach, for exemple, to the speed calculation (Lin, *et. al.*, 2001) and the metal transfer momentum of unidimensional form (Simpson and Zhu, 1995; Kovacevic, 1996; Zhang, 2000; Scotti and Rodrigues, 2009), multiple electrodes (Tusek, 1999), pulsed process (Vilarinho and Scotti, 2000; Richardson, *et. al.*, 1994), equivalent resistive-inductive circuit (Bingui, *et. al.*, 1998; Zhu, 1998; Saraev and Shipigunova, 1993; Reutzel, *et. al.*, 1995; Sudnik, *et. al.*, 2001), voltage drop (Quinn, *et. al.*, 1994; Bingul, *et. al.*, 2001; Quinn, 2002; Kim, 2001; Kim, 1991) and fume emission (Ioffe, *et. al.*, 1995; Haidar, 1999; Bosworth and Deam, 2000; Deam, *et. al.*, 2000; Mendez, *et. al.*, 2000; Redding, 2002; Dennis, *et. al.*, 2001).

Therefore, it can be stated that there are very sofisticated models available in the literature, but some of them demand large computational effort, which depend of correct set of physical properties dependent on temperature and actual boundary contitions imposed to solve the numeric simulation (Vilarinho, 2005). Thus, given these simplifications necessary to any model and starting from the assumption that a model more consolidated and practical are most interested for application to an industrial level, it is proposed to assess in this paper two models derived from Eq. (1) of Burn-off/original Melting Rate, called simplified model and expanded model. These models should be applied to the computation of the relationship between wire feed speed and current during GMAW process operating in conventional short-circuit for welding in mild steel groove joint in different shielding gases and positions in order to provide practical and usable results to industrial level.

2. MODELS

As discussed in the previous item, among the different existing models, this paper employs two models derived from Eq. (1), called simplified model and expanded model, described below. The main idea is to verify if the simplified model can assure appropriate estimation of the consumption relationship between wire feed speed and current, in comparison to a model more complete, which demands a more refined monitoring and calculation of electrical parameters.

2.1. Simplified Model

The first model shown in Eq (2) is extensively used and derived itself directly from Lesnewich's model, considering the process at steady state and no longer instantaneously.

$$WFS = \alpha I_M + \beta L I_{RMS}^2 \tag{2}$$

where WFS is the wire feed speed, I_M the mean current, L the energized length of electrode, I_{RMS} the root mean square current and α and β the parameters to be experimentally determined. Table 1 brings α and β values found in technical literature for mild steel during welding in flat position. Other values for different materials can be found on Bálsamo (2000) and Vilarinho (2000) references.

Table 1. Values for α and β determined by different autors for mild steel flat GMA welding.

References	Electrode Diameter [mm]	L [mm]	Shielding Gas	α [$m \cdot s^{-1} \cdot A^{-1}$]	β [$s^{-1} \cdot A^{-2}$]
Richardson, *et. al.* (1994)	0.8	15	$Ar+5\%CO_2+1,5\%O_2$	5.5E-04	35.0E-05
	1.0	15	$Ar+5\%CO_2+1,5\%O_2$	4.7E-04	9.10E-05
	1.2	15	$Ar+5\%CO_2+1,5\%O_2$	2.7E-04	5.9E-05
Dutra (1989)	1.0	10	$Ar+5\%CO_2$	2.65E-04	5.00E-05
Quintino and Allum (1984)	1.0	15	$Ar+5\%CO_2$	3.70E-04	5.64E-05
	1.2	15	$Ar+5\%CO_2$	3.10E-04	6.71E-05
Fujimura, *et. al.* (1987)	0.9	7.5 to 27.5	$Ar+20\%CO_2$	5.3E-04	1.7E-05
	1.2			3.1E-04	4.8E-05
	1.6			1.9E-04	1.5E-05

2.2. Expanded Model

As for the expanded model, it must consider the metal transfer influence. Thus, when considering the short-circuit transfer in GMAW process, two distinct periods/phases exist, namely open arc period/phase and short-circuit period/phase, as shown in Eq. (3).

$$WFS = \frac{t_A}{t_A + t_C}\left(\alpha I_{MA} + \beta_A L_A I_{RMSA}^2\right) + \frac{t_C}{t_A + t_C}\left(\beta_C L_C I_{RMSC}^2\right) \quad (3)$$

where t_A is the open arc mean time, t_C the short-circuit mean time duration, I_{RMSA} the RMS current in open arc phase, L_C the energized length of electrode in short-circuit phase, I_{RMSC} the RMS current in short-circuit phase and α, β_A and β_C the parameters to be determined.

During open arc, both heating due arc-electrode connection and Joule Effect exist. Therefore, the first parcel of Eq. (3) represents the open arc phase and it is weighted by his mean time (t_A) relative to total mean time (t_A+t_C). On the other hand, the second parcel represents the heating during short-circuit, where the main heating is given by Joule Effect. Thus, only the parcel represented by β_C parameter exists and it is weighted by short-circuit mean time (t_C) relative to mean time of both phases (t_A+t_C).

3. METHODOLOGY

The weldments were performed in a Motoman HP20 robot and a dedicated device developed to move the plate instead of the torch (which is conventionally fixed to robot's shock-absorber), according to Fig. 1. This option was adopted due the need for positional welding and the availability of fixing system of torch, with the possibility of change its position.

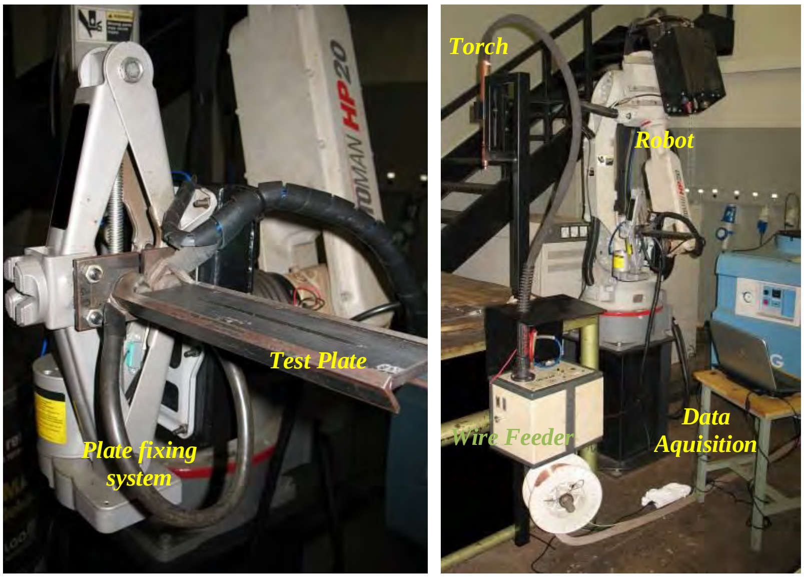

Figure 1. Experimental rig

A a constant voltage chopper power source was used and the weldments were carried out in flat, vertical down-downhill and overhead positions, varying the shielding gas between Ar+25%CO_2 e pure CO_2, which are the most common mixtures used to short-circuit GMAW. The gas output was set at 12 l/min. It was used AWS ER70S-6 wire electrode with 1.2 mm with travel angle of 90º and work angle of 0º. The base material is ABNT 1020, whose dimensions are shown in Fig. 2. The plate was milled simulating a V groove butt joint with no open root and face root of 2,35 mm, according to the same figure.

Initially, preliminary tests carried out to maintain the volume of deposited material constant (relationship between wire feed speed and travel speed), as well as three current ranges with allowance of ± 5 A. For that it was varied the contact tip to work distance (CTWD). The wire feed speed was set in three levels – 2.25, 2.86 and 3.46 m/min (and proportionally the travel speed), which led to the current ranges between 100-110 A, 135-145 A and 160-170 A. Each condition was repeated at least twice to check the repeatability and better statistical estimation.

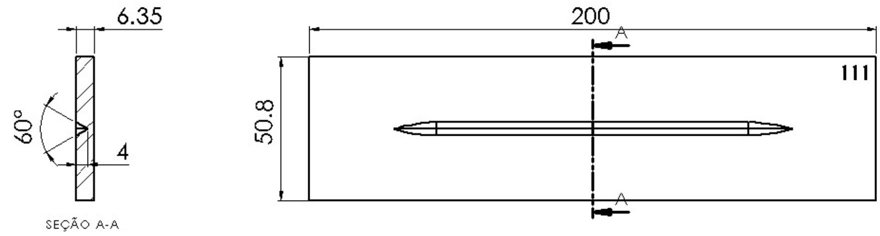

Figure 2: Dimensions and test plate lead up (measures in mm)

During the weldments, the necessary parameters for constants values estimation of Eq. (2) and Eq. (3) were monitored. It was used a data aquisition system (Machado, *et. al.*, 2012) set at 5 kHz for each channel for current and voltage monitoring and a dedicated software (Vilarinho and Araújo, 2012) for calculating the mentioned parameters. It was also used a high-speed camera and pre-established arc length criteria (Maia, 2001) to estimate the energized length of electrode. In order to achieve such estimation, for Eq. (1) the energized electrode length was assumed equal to the arc length during open-arc phase and for Eq. (2) the energized electrode length during short-circuit (L_C) was assumed equal to CTWD minus the reinforcement, measured after welding completion.

4. RESULTS AND DISCUSSION

From methodology proposed, preliminary tests was carried out to verify the current range possible to be obtained and from those was selected the parametric conditions of wire feed speed and CTWD. The employed values are shown for simplified model in Tab. 2 and Tab. 3 for Ar+25%CO_2 and 100%CO_2, respectively. For the expanded model, the measured values are shown at Tab. 4 and Tab. 5, respectively for the same shielding gases. It is emphasized that the current values in those tables appear with a decimal with the purpose of reduce the error spreading in measurement (α and β estimation), but the final value for current must be integer (with no decimal).

Table 1. Results for Ar+25%CO_2 in simplified model

Position	WFS [m/min]	I_M [A]	I_{RMS} [A]	L [mm]
Flat	2.25	107.8	121.9	9.50
		104.5	114.1	9.40
		104.3	113.0	9.11
		105.0	112.9	9.15
	2.86	141.9	152.2	9.59
		136.0	143.7	9.92
		136.6	144.4	9.88
		134.6	144.4	9.95
	3.46	170.3	190.9	9.65
		163.6	174.7	10.40
		160.8	168.6	10.64
		158.7	167.2	10.90
Downhill	2.25	105.5	121.7	8.35
		105.1	116.3	7.33
	2.86	140.0	153.1	10.49
		136.5	146.3	11.33
		133.1	144.0	8.00
	3.46	160.7	181.2	12.07
		162.1	173.2	12.07
		162.4	171.0	12.62
		157.7	169.2	12.62
Overhead	2.25	106.6	123.9	7.93
	2.86	133.4	162.3	8.26
		132.6	143.8	8.25
		133.0	141.4	7.68
	3.46	159.3	189.9	7.64
		159.5	187.6	6.83
		157.4	166.7	7.09
		159.7	169.8	6.24

ISSN 2176-5480

Table 2. Results for 100% CO_2 in simplified model

Posição	WFS [m/min]	I_M [A]	I_{RMS} [A]	L [mm]
Flat	2.25	110.6	130.6	8.54
		105.2	116.2	9.30
		102.6	116.2	7.73
		90.6	108.1	9.43
	2.86	134.8	175.1	7.47
		143.8	161.6	8.95
		141.8	152.0	9.41
		137.1	149.0	9.52
	3.46	152.9	191.5	9.91
		163.0	188.9	9.87
		153.4	174.4	10.36
		160.1	172.5	10.90
Downhill	2.25	115.4	135.4	9.24
		108.8	130.4	9.05
		102.0	118.7	9.15
	2.86	138.9	162.8	10.61
		140.0	160.7	11.37
		136.7	154.0	11.38
		133.3	150.0	11.21
	3.46	154.9	189.5	10.99
		160.1	186.2	10.97
		164.1	182.2	11.94
		159.0	175.3	12.21
Overhead	2.25	107.7	133.2	8.48
		105.6	127.9	1.70
	2.86	134.1	176.7	4.15
		133.0	175.7	2.23
		128.3	162.7	0.48
	3.46	152.5	203.0	5.89
		162.6	211.8	2.36
		157.5	197.4	1.66
		157.9	184.6	0.37

Table 3. Results for Ar+25%CO_2 in expanded model

Position	WFS [m/min]	t_A [ms]	t_C [ms]	L_A [mm]	L_C [mm]	I_{MA} [A]	I_{RMSA} [A]	I_{RMSC} [A]
Flat	2.25	12.15	3.49	9.50	10.30	124.7	117.6	137.8
		18.03	3.02	9.40	10.40	111.9	111.6	130.8
		37.16	2.94	9.11	10.31	111.7	110.2	146.5
	2.86	8.50	4.00	9.59	10.39	146.1	150.3	157.0
		10.74	3.11	9.92	10.92	142.4	142.8	147.9
		16.12	2.83	9.88	11.08	143.3	142.7	156.0
		37.97	3.34	9.95	11.35	134.9	140.9	181.6
	3.46	10.22	5.62	9.65	10.45	171.4	185.5	200.9
		10.05	3.65	10.40	11.40	168.1	172.0	182.7
		12.81	2.86	10.64	11.84	167.3	167.2	176.3
		21.71	2.86	10.90	12.30	164.7	164.7	187.0
Downhill	2.25	13.56	3.96	8.35	9.35	119.3	117.0	138.6
		19.32	3.18	7.33	8.53	115.7	113.4	135.2
	2.86	9.75	4.31	10.49	11.49	146.8	150.5	160.1
		11.69	3.78	11.33	12.53	139.7	145.1	151.5
		17.51	3.30	8.00	9.40	139.7	141.6	158.7
	3.46	10.53	5.32	12.07	13.07	163.1	179.3	185.4
		10.56	4.19	12.07	13.27	165.3	171.5	178.6
		12.36	3.59	12.62	14.02	164.8	170.6	173.8
		21.37	3.56	12.62	14.22	160.2	166.2	188.8
Overhead	2.25	14.24	3.77	7.93	9.13	126.7	118.1	145.8
	2.86	17.23	6.67	8.26	9.46	129.3	149.0	193.9
		13.43	3.22	8.25	9.65	142.3	141.0	157.2
		20.55	2.75	7.68	9.28	141.0	139.4	158.7
	3.46	19.27	6.44	7.64	8.84	155.1	175.3	229.1
		16.93	4.67	6.83	8.23	163.4	178.0	219.7
		15.85	2.70	7.09	8.69	168.1	164.3	182.6
		32.20	3.22	6.24	8.04	163.6	166.6	203.2

ISSN 2176-5480

Table 4. Results for 100% CO_2 in expanded model

Posição	WFS [m/min]	t_A [ms]	t_C [ms]	L_A [mm]	L_C [mm]	I_{MA} [A]	I_{RMSA} [A]	I_{RMSA} [A]
Flat	2.25	10.21	4.51	8.54	9.54	111.2	125.9	142.0
	2.25	10.72	2.77	9.30	10.50	109.3	115.1	121.6
	2.25	18.13	2.91	7.73	9.13	110.4	113.4	135.5
	2.86	21.02	9.77	7.47	8.47	111.4	154.1	215.8
	2.86	10.13	4.02	8.95	10.15	143.2	157.5	172.3
	2.86	10.35	2.57	9.41	10.81	148.9	151.0	157.4
	2.86	17.16	2.71	9.52	11.12	148.0	146.2	168.5
	3.46	15.64	7.67	9.91	10.91	141.8	179.3	215.6
	3.46	12.05	5.20	9.87	11.07	162.3	184.2	200.0
	3.46	12.76	3.62	10.36	11.76	158.3	170.2	189.7
	3.46	14.11	2.91	10.90	12.50	168.7	169.6	187.9
Downhill	2.25	10.46	4.95	9.24	10.44	114.8	131.8	144.1
	2.25	13.53	4.16	9.05	10.45	109.6	125.3	147.7
	2.25	19.15	3.31	9.15	10.75	108.6	114.6	142.7
	2.86	10.70	6.09	10.61	11.81	134.4	157.2	173.3
	2.86	11.45	5.03	11.37	12.77	135.8	156.9	170.6
	2.86	13.20	3.89	11.38	12.98	136.2	151.0	166.0
	2.86	17.35	3.51	11.21	13.01	133.6	146.6	168.8
	3.46	14.86	8.43	10.99	12.19	146.1	181.9	203.8
	3.46	12.45	5.95	10.97	12.37	154.3	180.9	198.4
	3.46	12.06	4.19	11.94	13.54	163.2	179.2	191.9
	3.46	16.50	3.83	12.21	14.01	158.2	171.7	192.2
Overhead	2.25	13.12	4.74	8.48	9.88	110.2	124.9	155.4
	2.25	15.60	3.55	1.70	3.30	111.8	122.6	151.0
	2.86	21.77	9.06	4.15	5.55	112.8	155.5	221.5
	2.86	24.67	7.45	2.23	3.83	119.4	157.4	227.9
	2.86	26.64	4.94	0.48	2.28	129.3	151.7	215.3
	3.46	25.10	11.15	5.89	7.29	128.4	175.0	257.6
	3.46	22.62	8.40	2.36	3.96	150.5	179.7	281.4
	3.46	24.06	5.90	1.66	3.46	152.8	173.9	274.0
	3.46	28.07	4.02	0.37	2.37	172.4	173.2	252.5

A first analysis to be made concerns the relationship of proportionality existing between wire feed speed and current, according to Fig. 3 and with more inference to Fig. 4 and Fig. 5 to the mean and RMS values, respectively. As previously discussed, this relationship is already described in technical literature and approximated by Eq. (2).

About the gas shielding influence in electrode consumption according to wire feed speed/current and welding position, it was noticed a little influence by Fig. 3. By performing an ANOVA, a little mean current influence was really noticed as shown in Fig. 4 with significant level p = 0.404, but for RMS current (Fig. 5) there is a higher statistical significance (p = 0.000). This low correlation with mean current is in accordance with previous work (Nascimento, *et. al.*, 2012), which demonstrated low influence for different mixes and both direct and inverse polarity. However, it is possible to observe that the mean current is higher for Ar+25%CO_2 blend, while RMS current is higher for 100% CO_2 case. Thus, by observing the melting rate equation, it leads to the conclusion that for the same wire feed speed, the blend is more correlated to heating effect during open arc time (Fig. 6); while 100% CO_2 is more correlated to heating effect during short-circuit (Fig. 7). Thus, the parcel relative to α constant (heating by arc-electrode connection) is higher for Ar+25%CO_2, while 100% CO_2 induces higher β (heating by Joule Effect), as will be follow shown.

About the results for current values shown at Fig. 3, the dispersion is higher for RMS current than the mean one, because the first term of burn-off rate (α term) is larger than the second term (β constant). Therefore, it is reasonable to assume that the mean current from first term have a more linear behavior and less dispersed than the ones observed for the RMS current, used in second term of the equation.

About the welding position, there was a trend of longer metal transfer in overhead position, as pointed out by the greatest open arc (Fig. 6) and short circuit (Fig. 7) times. This is due to de fact of more difficulty to accomplish the metal transfer due to gravity, which reduces the short-circuit rate (Fig. 8). The same behavior was observed in Fig. 8 for 100% CO_2, which also presents the tendency of reducing the frequency of short-circuit. It is due to the increase of its time duration, but with insignificant open arc time reduction in comparison to Ar+25%CO_2 blend.

Now with respect to the wire feed speed influence in open arc and short-circuit time, it is not possible to demonstrate a tendency, as shown in Fig. 6 and Fig. 7. It would be expected a short-circuit rate increase by necessity to increase the quantity of metal transferred by travel speed increase, which would take to a reduction in the metal transfer time. In this case, it was kept this rate approximately constant (Fig. 8) considering the quantity of metal transferred (droplet volume) increased at each performed transfer.

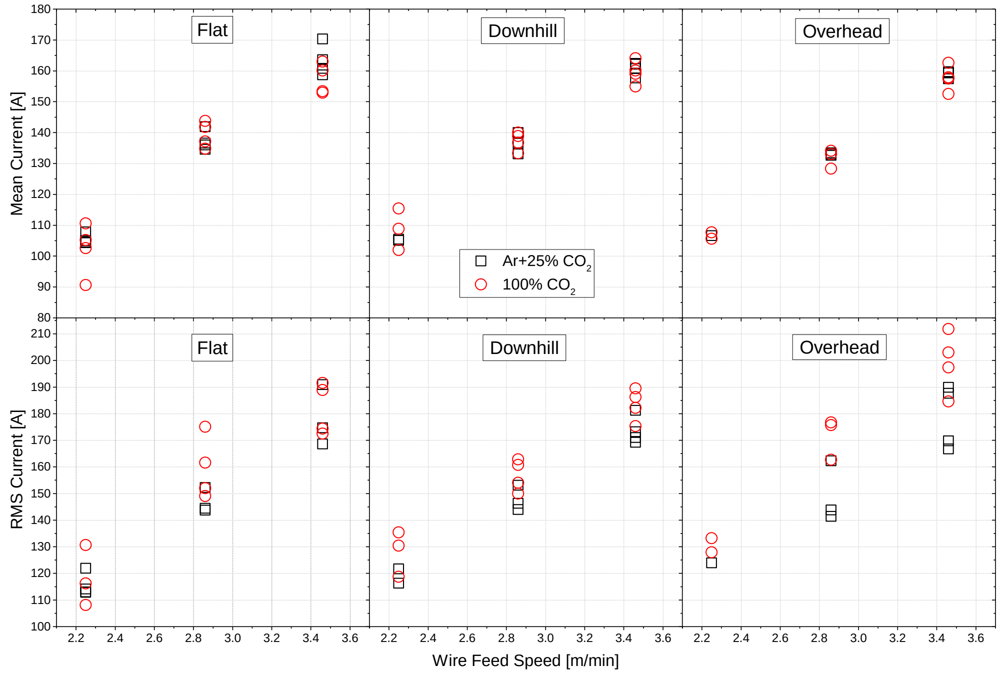

Figure 1. Relationship between current, wire feed speed, shielding gas and welding position

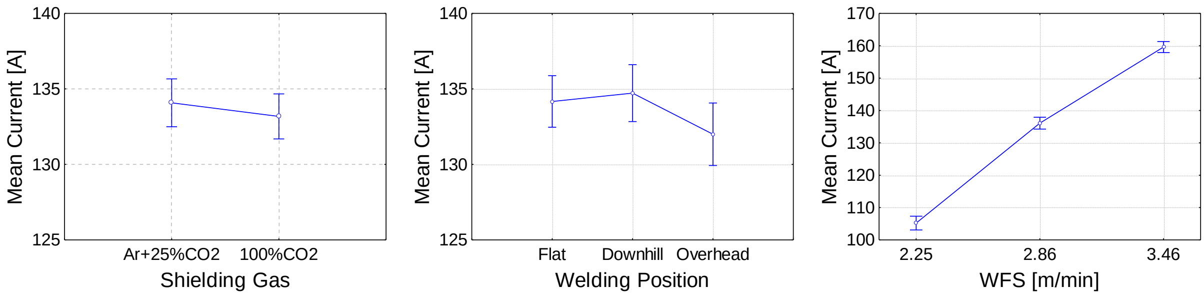

Figure 2. Influence of welding parameters on the mean curent

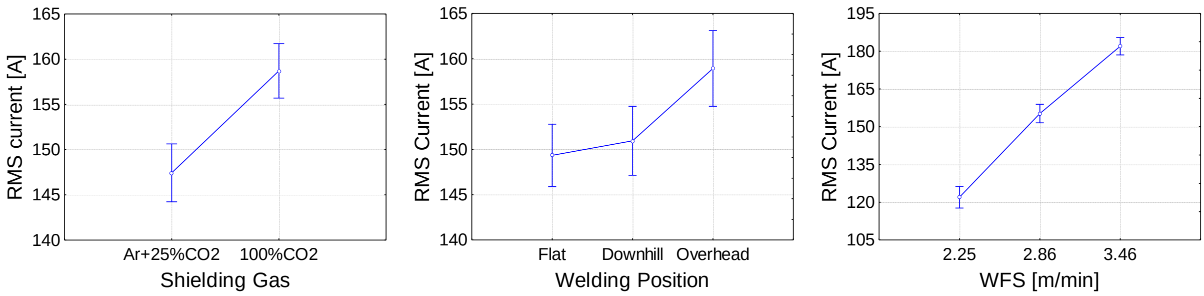

Figure 3. Influence of welding parameters in RMS current

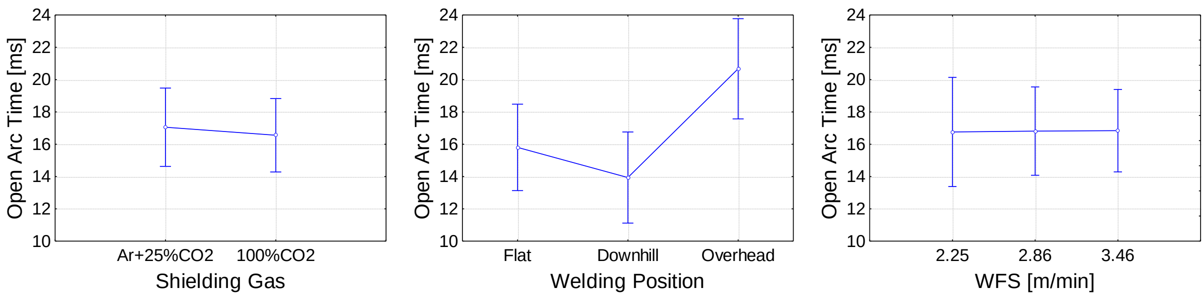

Figure 4. Influence of welding parameters in open arc time

ISSN 2176-5480

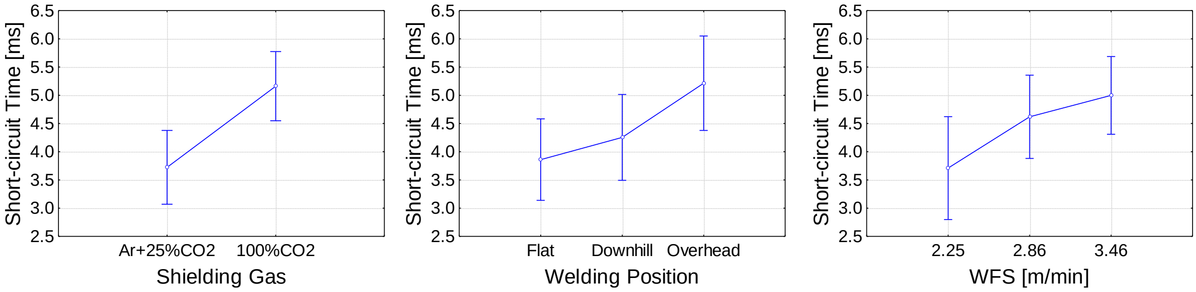

Figure 5. Influence of welding parameters in short-circuit time

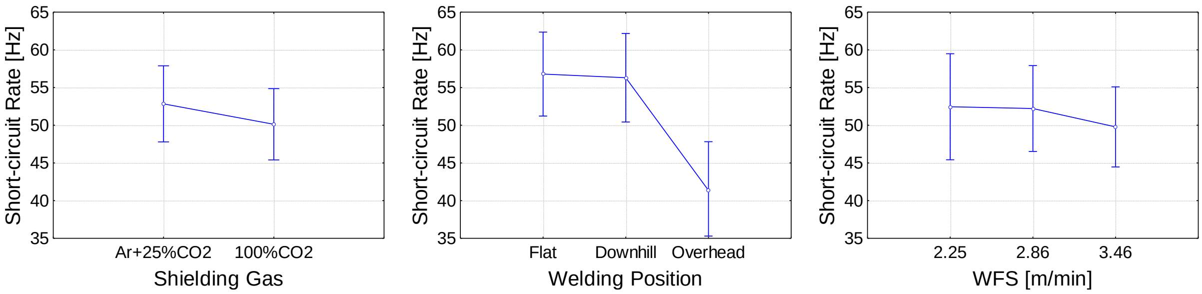

Figure 6. Influence of welding parameters in short-circuit rate

By using non-linear regression based on models from Eq. (2) and (3), its parameters were calculated as shown in Tab. 6. These models shown values of R^2 equals to 0.985 and 0.992 for simplified and expanded models, respectively. In addition the model's statistical significance level (p) ranged between 0.029 and 0.016 for simplified and expanded ones, respectively. This demonstrates that both models represents adequately (reliability less than 0.05) the phenomenon investigated, with results slightly better (better fit and reliability) for expanded model. It is emphasized that these values are generally in accordance with those presented in Tab. 1. One point that draws attention is the presence of negative values for β constant. This reflects the fact that the model is a statistical regression (curve fitting), but also denotes the minor of the Joule Effect against arc-electrode connection heating. Vilarinho (2000) also mentions negative values for β, although it is more commom for materials with low electrical resistivity like aluminum.

Table 5. Burn-off rate constants obtained by both models

Shielding Gas	Position	Simplified Model		Expanded Model		
		α [m·s^{-1}·A^{-1}]	β [s^{-1}·A^{-2}]	α [s^{-1}·A^{-2}]	β_A [s^{-1}·A^{-2}]	β_A [s^{-1}·A^{-2}]
Ar+25%CO_2	Flat	3.59E-04	-4.50E-06	3.37E-04	1.14E-05	1.29E-04
	Downhill	3.48E-04	3.75E-06	3.56E-04	-5.18E-08	1.28E-04
	Overhead	3.58E-04	1.66E-06	2.46E-04	1.15E-04	8.22E-05
100%CO_2	Flat	3.17E-04	2.15E-05	3.85E-04	-3.99E-05	1.81E-04
	Downhill	3.20E-04	1.62E-05	3.79E-04	-1.96E-05	1.44E-04
	Overhead	3.61E-04	1.72E-06	3.90E-04	-9.44E-05	2.49E-04

From α and β coefficients shown at Tab. 6, it is possible to state higher values of α are achieved for Ar+25%CO_2 shielding gas, whereas the β constant is higher for 100%CO2, as discussed earlier according to higher heating of arc-electrode connection (for mix shielding gas) or by Joule Effect (pure CO_2).

For the welding position, it was not possible to identify characteristic tendency, since there are correlations between current, open arc time and short-circuit time (and both last in metal transfer rate). As previously discussed, the welding position had stronger effect in these parameters than burn-off rate constants.

Finnally, the applicability of both models must be discussed in terms of lower error in to estimate correctly the wire feed speed to a given required current, since the power source was operating in constant-voltage mode and the current is a consequence of the set of the wire feed speed. Therefore, an analisys based on obtained residuals was done for both models. Tables 7 and 8 bring the obtained residuals for each welding conditions according to models, welding positions and shielding gases. By performing an ANOVA in those residuals it is possible to check the dispersion level found (Fig. 9) and welding position and shielding gases influences used for both models (Fig. 10 and Fig. 11).

From these results, it is possible to assert that expanded model shown consistently lower results than simplified one for residual levels. Although the significance level (p = 0.518, as shown in Fig. 9) did not indicated directly the estimation advantage and consequent reduction of residual by expanded model, the obtained values with this models are in fact lower. Special attention must be given to overhead position, where the estimation tendendy is reversed, in other words, the simplified model got slicely lower residual level than expanded one, as shown in Fig. 10. However, this difference is smoother than the one observed to other positions, as seen in the same figure. Thus, in general, the expanded model enabled the correct wire feed speed estimation with lower residual levels, with great fitting (R^2 = 0.992) with righ statistical significance (p = 0.016).

Table 6. Residual level comparison between models for Ar+25%CO_2 shielding gas.

Position	WFS [m/min]			Resídual [m/min]	
	Fit	Simplified Model	Expanded Model	Simplified Model	Expanded Model
Flat	2.25	2.28	2.36	-0.03	-0.11
	2.25	2.22	2.20	0.03	0.05
	2.25	2.21	2.29	0.04	-0.04
	2.25	2.23	2.74	0.02	0.12
	2.86	3.00	2.75	-0.14	0.11
	2.86	2.87	2.89	-0.01	-0.03
	2.86	2.89	2.86	-0.03	0.00
	3.46	3.57	3.54	-0.11	-0.08
	3.46	3.44	3.43	0.02	0.03
	3.46	3.38	3.45	0.08	0.01
	3.46	3.34	3.50	0.12	-0.04
	Quadratic average of residuals			0.24	0.23
Downhill	2.25	2.23	2.29	0.02	-0.04
	2.25	2.22	2.29	0.03	-0.04
	2.86	2.98	2.87	-0.12	-0.01
	2.86	2.91	2.80	-0.05	0.06
	2.86	2.82	2.80	0.04	0.06
	3.46	3.45	3.47	0.01	-0.01
	3.46	3.47	3.45	-0.01	0.01
	3.46	3.48	3.46	-0.02	0.00
	3.46	3.38	3.49	0.08	-0.03
	Quadratic average of residuals			0.17	0.11
Overhead	2.25	2.30	2.28	-0.05	-0.03
	2.86	2.89	2.78	-0.03	0.07
	2.86	2.87	2.84	-0.01	0.03
	2.86	2.87	2.88	-0.01	-0.02
	3.46	3.45	3.51	0.01	-0.04
	3.46	3.45	3.49	0.01	-0.02
	3.46	3.40	3.46	0.06	0.00
	3.46	3.45	3.43	0.01	0.03
	Quadratic average of residuals			0,09	0,10

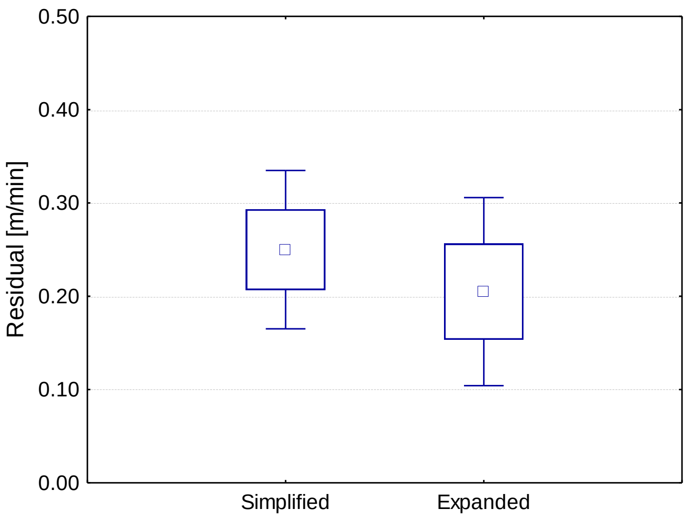

Figure 7. Residual levels obtained from both models with statistical significance p = 0.518

ISSN 2176-5480

Table 7. Residual level comparison between models for 100% CO_2 shielding gas.

Position	WFS [m/min]			Resídual [m/min]	
	Fit	Simplified Model	Expanded Model	Simplified Model	Expanded Model
Flat	2.25	2.29	2.20	-0.04	0.05
	2.25	2.16	2.12	0.09	0.13
	2.25	2.08	2.25	0.17	0.00
	2.86	2.86	2.83	0.00	0.03
	2.86	3.03	2.92	-0.17	-0.06
	2.86	2.97	2.93	-0.11	-0.07
	2.86	2.88	3.00	-0.02	-0.14
	3.46	3.37	3.50	0.09	-0.04
	3.46	3.55	3.51	-0.09	-0.05
	3.46	3.32	3.31	0.14	0.15
	3.46	3.46	3.43	0.00	0.03
	Quadratic Average of Residuals			0.34	0.28
Downhill	2.25	2.38	2.25	-0.13	0.00
	2.25	2.23	2.24	0.02	0.01
	2.25	2.08	2.27	0.17	-0.02
	2.86	2.94	2.86	-0.08	0.00
	2.86	2.97	2.90	-0.11	-0.04
	2.86	2.88	2.86	-0.02	0.00
	2.86	2.80	2.83	0.06	0.03
	3.46	3.35	3.43	0.11	0.03
	3.46	3.44	3.45	0.02	0.01
	3.46	3.53	3.53	-0.07	-0.07
	3.46	3.41	3.42	0.05	0.04
	Quadratic Average of Residuals			0.29	0.10
Overhead	2.25	2.35	2.33	-0.10	-0.08
	2.25	2.29	2.22	-0.04	0.03
	2.86	2.92	2.66	-0.06	0.20
	2.86	2.89	2.59	-0.03	0.27
	2.86	2.78	2.73	0.08	0.13
	3.46	3.33	3.60	0.13	-0.14
	3.46	3.54	3.50	-0.08	-0.04
	3.46	3.42	3.40	0.04	0.06
	3.46	3.43	3.74	0.03	-0.28
	Quadratic Average of Residuals			0.37	0.41

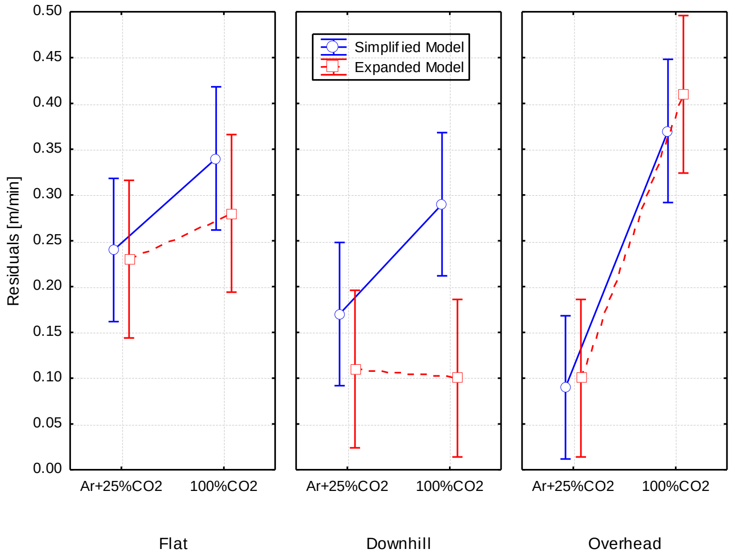

Figure 8. Influence of shielding gas in order to welding position in residual level for both models

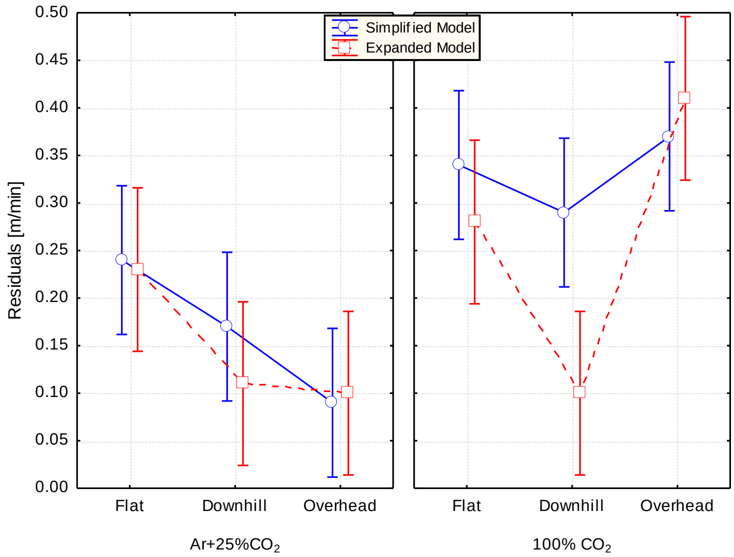

Figure 9. Influence of welding position in order to shielding gas in residual level for both models

5. CONCLUSIONS

From obtained and discussed results in experimental consitions presented, it is possible to conclude that:

- The expanded model enabled better experimental fitting ($R^2 = 0.992$) with lower residual and higher statistical significance ($p = 0.016$), and therefore it must be used in GMAW process with short-circuit transfer;
- Higher values of α constant are achieved for Ar+25%CO_2 blend, although the β constant is higher for pure CO_2. Despite to welding position, it is not possible identify characteristic trend. Thus, the blend is more correlated to heating during arc open time, whereas pure CO_2 is more correleated to heating by short-circuit;
- The results dispersion was higher for RMS current than mean. Thus, is reasonable to assume that mean current present in first term of burn-rate has a more straight behavior and less scattered than RMS current, used in second term of the same equation;
- About the welding position, there was a trend to lower metal transfer rate in overhead position, with higher both open arc and short-circuit times;
- The pure CO_2 also shown trend in reduce the short-circuit rate by meaningful increase of short-circuit duration time, but with negligible open arc time reduction in comparison to the Ar+25%CO_2 blend.

6. ACKNOWLEDGEMENTS

The authors would like to thank to Fapemig (under Proc. TEC-PPM-00511-12), to CNPq (under Procs. 481975/2012-8 and 307710/2011), to Laprosolda/UFU, to CTBC/Algar Telecom and to CAPES/PROEX.

7. REFERENCES

ALLUM, C.J. Metal Transfer in Arc Welding as a Varicose Instability: I. Varicose Instabilities in a Current-carrying Liquid Cylinder with Surface Charge. J. Phys. D: Appl. Phys., v.18, p. 1431-1446, 1985.

ALLUM, C.J. Metal Transfer in Arc Welding as a Varicose Instability: II. Development of Model for Arc Welding. J. Phys. D: Appl. Phys., v.18, p. 1447-1468, 1985.

AMSON, J.C. An Analysis of the Gas-shielded Consumable Metal Arc Welding System. British Welding Journal, v.April, p. 232-249, 1962.

AMSON, J.C. Lorentz Force in the Molten Tip of an Arc Electrode. British Journal of Applied Physics, v.16, p. 1169-1179, 1965.

BÁLSAMO, P.S.S., Desenvolvimento de um Sistema Sinérgico Não Linear para Soldagem MIG Pulsado de Aço Inoxidável. 2000, Universidade Federal de Uberlândia. p. 205.

BINGUL, Z., G.E. COOK, and A.M. STRAUSS. Dynamic Model for Electrode Melting Rate in Gas Metal Arc Welding Process. Science and Technology of Welding and Joining, v.6, n. 1, p. 41-50, 2001.

BINGUL, Z., et. al. An Investigation of Constant Potential GMAW Instability Behavior. Proceed. 5th Int. Conf. Trends in Welding Research, v., p. 289-294, 1998.

BOSWORTH, M.R. and R.T. DEAM. Influence of GMAW Droplet Size on Fume Formation Rate. J. Phys. D: Appl. Phys., v.33, p. 2605-2610, 2000.

CHOI, S.K., Y.-S. KIM, and C.D. YOO. Dimensional Analysis of Metal Transfer in GMA Welding. J. Phys. D: Appl. Phys., v.32, p. 326-334, 1999.

CHOI, J.H., J.Y. LEE, and C.D. YOO. Dynamic Force Balance Model for Metal Transfer Analysis in Arc Welding. J. Phys. D: Appl. Phys., v.34, p. 2658-2664, 2001.

CHOI, S.K., C.D. YOO, and Y.-S. KIM. Dynamic Simulation of Metal Transfer in GMAW, Part 1: Globular and Spray Transfer Modes. Welding Journal, v.January, p. 38s-44s, 1998.

CHOI, S.K., C.D. YOO, and Y.-S. KIM. Dynamic Simulation of Metal Transfer in GMAW, Part 1: Short-circuit Mode. Welding Journal, v.January, p. 45s-51s, 1998.

CHOI, S.K., C.D. YOO, and Y.-S. KIM. The Dynamic Analysis of Metal Transfer in Pulsed Current Gas Metal Arc Welding. J. Phys. D: Appl. Phys., v.31, p. 207-215, 1998.

DEAM, R.T., S.W. SIMPSON, and J. HAIDAR. A Semi-empirical Model of the Fume Formation from Gas Metal Arc Welding. J. Phys. D: Appl. Phys., v.33, p. 1393-1402, 2000.

DENNIS, J.H., et al. A Model for Prediction of Fume Formation Rate in Gas Metal Arc Welding (GMAW), Globular and Spray Modes, DC Electrode Positive. Ann. Occup. Hyg., v.45, n. 2, p. 105-113, 2001.

DUTRA, J.C. Procedimento Computadorizado do estudo de Transferência Metálica para a Determinação das Variáveis de Soldagem com Corrente Pulsada. XV ENTS, São Paulo, v., p. 637-652, 1989.

FAN, H.G. and R. KOVACEVIC. Droplet Formation, Detachment, and Impingement on the Molten Pool in Gas Metal Arc Welding. Metallurgical and Materials Transactions B, v.30B, n. August, p. 791-801, 1999.

FAN, H.G. and R. KOVACEVIC. Dynamic Analysis of Globular Metal Transfer in Gas Metal Arc Welding – a Comparison of Numerical and Experimental Results. J. Phys. D: Appl. Phys., v.31, p. 2829-2941, 1998.

FUJIMURA, H., E. IDE, and H. INOUE. Estimation of Contact Tip-workpiece Distance in Gas Shielded Metal Arc Welding. Quarterly Journal of Japan Welding Society, v., p. 522-528, 1987.

HAIDAR, J. An Analysis of the Formation of the Metal Droplets in Arc Welding. J. Phys. D: Appl. Phys., v.31, p. 1233-1244, 1998.

HAIDAR, J. An Analysis of Heat Transfer and Fume Production in Gas Metal Arc Welding. III. J. Appl. Phys., v.85, n. 7, p. 3448-3459, 1999.

HAIDAR, J. Predictions of Metal Droplet Formation in Arc Welding. J. Phys. D: Appl. Phys., v.84, n. 7, p. 3530-3540, 1998.

HIRT, C.W.A.N., B.D. Volume of Fluid (VOF) Method for the Dynamics of Free Boundaries. Journal of Computational Physics, v.39, p. 201-225, 1981.

IOFFE, I., et al. Fume Formation Rate at Globular to Spray Mode Transition during Welding. J. Phys. D: Appl. Phys., v.28, p. 2473-2477, 1995.

JONES, L.A., Dynamic Electrodes Forces in Gas Metal Arc Welding. 1996, MIT. p. 313.

JONES, L.A., T.W. EAGAR, and J.H. LANG. A Dynamic Model of Drops Detaching from a Gas Metal Arc Welding Electrode. J. Phys. D: Appl. Phys., v.31, p. 107-123, 1998.

JONES, L.A., T.W. EAGAR, and J.H. LANG. Magnetic Forces Acting on Molten Drops in Gas Metal Arc Welding. J. Phys. D: Appl. Phys., v.31, p. 93-10, 1998.

KIM, Y.-S., Metal Transfer in Gas Metal Arc Welding. 1989, MIT. p. 294.

KIM, C.-H.A.N., S-J., . A Study of an Arc Sensor Model for Gas Metal Arc Welding with Rotating Arc. Part I: Dynamic Simulation of Wire Melting. Proc. Instn. Mech. Engrs., v.215, n. Part B, p. 1271-1279, 2001.

KIM, Y.-S. and T.W. EAGAR. Analysis of Metal Transfer in Gas Metal Arc Welding. Welding Journal, v.June, p. 269s-278s, 1993.

KIM, Y.-S., D.M. MCELIGOT, and T.W. EAGAR. Analyses of Electrode Heat Transfer in Gas Metal Arc Welding. Welding Journal, v.January, p. 20s-31s, 1991.

KOVACEVIC, R., et al. Dynamics of Droplet Geometry During Metal Transfer in GMAW – a Model for Process Control. Advanced Materials: Development, Characterization, Processing and Mechanical Behaviour, v.MD-Vol. 74, p. 143-144, 1996.

LANCASTER, J.F. The Physics of Welding. Pergamon Press & International Institute of Welding, 1986. 340 p.

LESNEWICH, A. Control of Melting Rate and Metal Transfer in Gas-shielded Metal-arc Welding. Part I – Control of Electrode Melting Rate. Welding Journal, v.August, p. 343s-353s, 1958.

LESNEWICH, A. Control of Melting Rate and Metal Transfer in Gas-shielded Metal-arc Welding. Part II – Control of Metal Transfer. Welding Journal, v.August, p. 418s-425s, 1958.

LIN, Q., X. LI, and S.W. SIMPSON. Metal Transfer Measurements in Gas Metal Arc Welding. J. Phys. D: Appl. Phys., v.34, p. 647-353, 2001.

LOWKE, J.J. Simple Model for the Transition Current from Globular to Spray Transfer in Gas Metal Arc Welding. Australasian Welding Journal, v.42, p. 32-35, 1997.

MACHADO, M.V.R., et al. Sistema embarcado para monitoramento sem fio de sinais em soldagem a arco elétrico com abordagem tecnológica. Soldagem e Inspeção, v.17, p. 147-157, 2012.

MAIA, T.C.G., Utilização de Técnicas de Processamento Digital de Imagens no Estudo de Transferência Metálica em Soldagem a Arco Voltaico. 2001, Universidade Federal de Uberlândia. p. 124.

ISSN 2176-5480

MENDEZ, P.F., N.T. JENKINS, and T.W. EAGAR. Effect of Electrode Droplet Size on Evaporation and Fume Generation in GMAW. Proceedings of the Gas Metal Arc Welding for the 21st Century Conference - Orlando - December 6-8, v., p. 2000.

NASCIMENTO, A.S., L.C. MENEZES JUNIOR, and L.O. VILARINHO. Efeito do formato de onda e gás de proteção sobre a taxa de fusão e geometria do cordão na soldagem MIG/MAG-PV. Soldagem & Inspeção, v.17, p. 40-48, 2012.

NEEDHAM, J.C., C.J. COOKSEY, and D.R. MILNER. Metal Transfer in Inert-gas Shielded-arc Welding. British Welding Journal, v.7, n. 2, p. 101-114, 1960.

NEMCHINSKY, V.A. Electrode Melting during Arc Welding with Pulsed Current. J. Phys. D: Appl. Phys., v.31, p. 2797-2802, 1998.

NEMCHINSKY, V.A. Heat Transfer in an Electrode during Arc Welding with a Consumable Electrode. J. Phys. D: Appl. Phys., v.31, p. 730-736, 1998.

NEMCHINSKY, V.A. The Rate of Melting of the Electrode during Arc Welding. The Influence of Discrete Removal of the Melt. J. Phys. D: Appl. Phys., v.31, p. 1565-1569, 1998.

NORRISH, J. and I.F. RICHARDSON. Metal Transfer Mechanisms. Welding & Metal Fabrication, v.January/February, p. 17-22, 1988.

QUINN, T.P. Process Sensitivity of GMAW: Aluminum vs. Steel. Welding Journal, v.April, p. 55s-60s, 2002.

QUINN, T.P., R.B. MADIGAN, and T.A. SIEWERT. An Electrode Extension Model for Gas Metal Arc Welding. Welding Journal, v.October, p. 241s-248s, 1994.

QUINTINO, L. and C.J. ALLUM. Pulsed GMAW: interactions between process parameters – Part 1. Welding and Metal Fabrication., v.March, p. 5, 1984.

REDDING, C.J. Fume Model for Gas Metal Arc Welding. Welding Journal, v.June, p. 95s-103s, 2002.

REUTZEL, E.W., et al. Derivation and Calibration of a Gas Metal Arc Welding (GMAW) Dynamic Droplet Model. Trends in Welding Research, v., p. 377-384, 1995.

RICHARDSON, I.M., P.W. BUCKNALL, and I. STARES. The Influence of Power Source Dynamics on Wire Melting Rate in Pulsed GMA Welding. Welding Journal, v.February, p. 32s-37s, 1994.

SARAEV, Y.N. and O.I. SHPIGUNOVA. A Mathematical Model of Melting and Transfer of Electrode Metal with Systematic Short-circuiting of the Arc Gap. Welding International, v.4, n. 10, p. 793-797, 1993.

SCOTTI, A. and C.E.A.L. RODRIGUES. Determination of momentum as a mean of quantifying the mechanical energy delivered by droplets during MIG/MAG welding. Eur. Phys. J. Appl. Phys., v.45, p. 2009.

SIMPSON, S.W. and P. ZHU. Formation of Molten Droplets at a Consumable Anode in an Electric Welding Arc. J. Phys. D: Appl. Phys., v.28, p. 1594-1600, 1995.

SUDNIK, V.A., A.V. IVANOV, and W. DILTER. Mathematical Model of a Heat Source in Gas-shielded Consumable Electrode Arc Welding. Welding International, v.15, n. 2, p. 146-152, 2001.

TUSEK, J. A Mathematical Model for the Melting Rate in Welding with a Multiple-wire Electrode. J. Phys. D: Appl. Phys., v.32, p. 1739-1744, 1999.

VILARINHO, L.O. Characterisation of TIG Arc Structures by Using Experimental Techniques. Cranfield University, 2002, p. 325

VILARINHO, L.O., Desenvolvimento e Avaliação de um Algoritmo Alternativo para Soldagem MIG Sinérgica de Alumínio. 2000, Universidade Federal de Uberlândia. p. 120.

VILARINHO, L.O. Welding Arc Modelling: a Survey. Soldagem & Inspeção, v.10, n. 1, p. 38-46, 2005.

VILARINHO, L.O. and D.B. ARAÚJO, Programa Curto-circuito para cálculo de IVcc, U.F.d. Uberlândia, Editor. 2012: Brasil.

VILARINHO, L.O., A.V. COSTA, and A. SCOTTI. A Contribution to Numerical and Experimental Determination of Electrode Temperature and Voltage Drop during GMAW. Soldagem & Inspeção, v.10, n. 2, p. 92-99, 2005.

VILARINHO, L.O. and A. SCOTTI. An Alternative Algorithm for Synergic Pulsed GMAW of Aluminium. Australasian Welding Journal, v.45, p. 36-44, 2000.

WANG, G., G. HUANG, and Y.M. ZHANG. Numerical Analysis of Metal Transfer in Gas Metal Arc Welding. Metallurgical and Materials Transactions B, v.34B, n. June, p. 345-353, 2003.

WASZINK, J.H. and L.H.J. GRAAT. Experimental Investigation of the Forces Acting on a Drop of Weld Metal. Welding Journal, v.April, p. 108s-116s, 1983.

WASZINK, J.H. and M.J. PIENA. Experimental Investigation of Drop Detachment and Drop Velocity in GMAW. Welding Journal, v.November, p. 289s-298s, 1986.

WASZINK, J.H. and G.J.P.M. VAN DEN HEUVEL. Heat Generation an Heat Flow in the Filler Metal in GMA Welding. Welding Journal, v.August, p. 269s-282s, 1982.

WATKINS, A.D., H.B. SMARTT, and J.A. JOHNSON. A Dynamic Model of Droplet Growth and Detachment in GMAW. Int. Trends in Welding Science and Technology, v., p. 993-997, 1992.

ZHU, P. Computer Simulation of Gas Metal Arc Welding Arcs. Proceed. 5th Int. Conf. Trends in Welding Research, v., p. 283-288, 1998.

ZHANG, Y.M.A.L., E., . Numerical Analysis of the Dynamic Growth of Droplets in Gas Metal Arc Welding. Proc. Instn. Mech. Engrs., v.214, n. Part C, p. 1247-1258, 2000.